

TITLE: SIMULATION STUDIES OF THE LAMPF PROTON LINAC

AUTHOR(S): R. W. Garnett AOT-1
E. R. Gray AOT-1
L. J. Rybarcyk AOT-6
T. P. Wangler AOT-1

SUBMITTED TO: 1995 Particle Accelerator Conference and International Conference
On High-Energy Accelerators
May 1-5, 1995, Dallas, Texas

Los Alamos
NATIONAL LABORATORY

Los Alamos National Laboratory, an affirmative action/equal opportunity employer, is operated by the University of California for the U.S. Department of Energy under contract W-7405-ENG-36. By acceptance of this article, the publisher recognizes that the U.S. Government retains a nonexclusive, royalty-free license to publish or reproduce the published form of this contribution, or to allow others to do so, for U.S. Government purposes. The Los Alamos National Laboratory requests that the publisher identify this article as work performed under the auspices of the U.S. Department of Energy.

Form No. 836 RS
ST 2629 1091

DISTRIBUTION OF THIS DOCUMENT IS UNLIMITED

MASTER

SIMULATION STUDIES OF THE LAMPF PROTON LINAC

R. W. Garnett, E. R. Gray, L. J. Rybarczyk, and T. P. Wangler
Accelerator Operations and Technology Division,
Los Alamos National Laboratory, Los Alamos, NM 87545 USA*

I. INTRODUCTION

The LAMPF accelerator consists of two 0.75-MeV injectors, one for H^+ and the other for H^- , a separate low-energy beam transport (LEBT) line for each beam species, a 0.75 to 100-MeV drift-tube linac (DTL) operating at 201.25-MHz, a 100-MeV transition region (TR), and a 100 to 800-MeV side-coupled linac (SCL) operating at 805-MHz. Each LEBT line consists of a series of quadrupoles to transport and transversely match the beam. The LEBT also contains a prebuncher, a main buncher, and an electrostatic deflector. The deflector is used to limit the fraction of a macropulse which is seen by the beam diagnostics throughout the linac. The DTL consists of four rf tanks and uses singlet FODO transverse focusing. The focusing period is doubled in the last two tanks by placing a quadrupole only in every other drift-tube. Doublet FDO transverse focusing is used in the SCL. The TR consists of separate transport lines for the H^+ and H^- beams. The pathlengths for the two beams differ, by introducing bends, so as to delay arrival of one beam relative to the other and thereby produce the desired macropulse time structure. Peak beam currents typically range from 12 to 18-mA for varying macropulse lengths which give an average beam current of 1-mA. The number of particles per bunch is of the order 10^8 .

The work presented here is an extension of our previous work [1]. We have attempted to do a more complete simulation by including modeling of the LEBT. No measurements of the longitudinal structure of the beam, except phase-scans, are performed at LAMPF. Transverse measurements include slit and collector emittance measurements and wire scans to determine beam size and centroids. We will show that, based on simulation results, the primary causes of beam spill are inefficient longitudinal capture and the lack of longitudinal matching. Measurements to support these claims are not presently made at LAMPF. However, agreement between measurement and simulation for the transverse beam properties and transmissions serve to benchmark the simulations.

II. SIMULATION TECHNIQUES

The LEBT, DTL, and TR were modeled using the PARMILA code. All simulations began with an initial distribution of either 10,000 or 100,000 macroparticles. The transverse beam was generated as a Gaussian distribution in 4-D phase space and was truncated at 3σ . The longitudinal distribution was generated with zero energy spread and $\pm 180^\circ$ phase spread. Simulations were done separately for H^+ and H^- , and were started at the center of the prebuncher in the LEBT. This was done because there are no longitudinal emittance measurements made at LAMPF. The beam was initially propagated to the center of the endwall quadrupole of the first tank of the DTL. The initial input beam parameters at the prebuncher center were determined by using the TRACE 3-D code to determine the input match to the DTL for the measured beam current and emittances, and tracing back to the prebuncher center. The prebuncher and main buncher voltages used in the simulations were those derived for the actual cavities from Q-measurements and SUPERFISH calculations. The prebuncher and main buncher voltages were 2.8 kV and 8.2 kV, respectively. Because the level of space charge neutralization in the LEBT is unknown and no measurements of longitudinal beam parameters are made, there is some uncertainty in the conditions in the LEBT. A comparison between the simulation results and transverse emittance measurements made just downstream of the prebuncher and just upstream of the first DTL tank was made. We examined the effect of space-charge in the LEBT, however, the best agreement between simulations and measurements was achieved when a fully neutralized beam was assumed in the LEBT and an iterative procedure to determine the initial transverse beam Twiss parameters (α, β) at the prebuncher center was used. Since emittance measurements are made with the deflector on, it is not unreasonable to assume that the beam may be nearly fully neutralized in the region of the deflector because most of each macropulse is dumped on the surface of the deflector cavity structure to avoid damage to the emittance measuring gear at higher beam energies.

At LAMPF, the operators generally reduce the DTL tank r.f. amplitudes below the design values in order to reduce beam spill in the SCL above 100-MeV. The 1993 relative r.f. amplitudes, as determined from power measurements, were 0.934, 0.938, 0.90, and 0.981 of the design amplitudes for tanks 1-4, respectively. These settings were used in the simulations when comparing to measurements taken under nominal operating conditions.

*Work supported by Los Alamos National Laboratory Directed Research and Development, under the auspices of the United States Department of Energy.

The output distributions from the PARMILA simulations were used as input for the coupled-cavity code, CCLDYN. The SCL design values for r.f. amplitudes and quadrupole gradients were used in the simulations. Measured misalignments for tanks and magnets in the SCL were not used.

III. COMPARISON WITH MEASUREMENTS

A. H^+ Beam Simulation

Table 1 shows the results of both measurements and simulations for the H^+ beam. The measured emittance values were obtained by the slit and collector method. These measurements were made at the entrance to the DTL (0.75-MeV) and in the TR (100-MeV). No emittance measurements were recorded at 800-MeV for this study. There is reasonable agreement between measurements and simulations for the emittance values and excellent agreement for transmission through the DTL.

Table 1 - H^+ 100-MeV Measurement and Simulation Results.

	Measured	Simulated
$\epsilon_x(\pi - \text{cm} - \text{mrad}, \text{rms}, \text{norm})$	0.026	0.038
$\epsilon_y(\pi - \text{cm} - \text{mrad}, \text{rms}, \text{norm})$	0.020	0.0184
$\epsilon_{x-\text{out}} / \epsilon_{x-\text{in}}$	4.2	9.7
$\epsilon_{y-\text{out}} / \epsilon_{y-\text{in}}$	5.3	4.7
DTL Transmission	67%	70%

B. H^- Beam Simulation

The two LEBT lines (H^+ and H^-) converge into one single line with the two beams bent by a common dipole magnet. There is an aperture restriction in the H^- beam line just before the convergence point. Downstream of the dipole magnet are four quadrupoles which are adjusted to match the H^+ beam into the DTL. The tuning of the H^- beam is a compromise between maximizing transmission through the aperture restriction and its match to the DTL. This is accomplished by varying the settings of quadrupoles which are upstream of the dipole magnet. Emittance growth of the H^- beam is observed due to the transverse mismatch at injection to the DTL. Table 2 shows the results of both measurements and simulations for the H^- beam at 100-MeV. The measured emittance growth is larger than that determined from the simulations by using the nominal operating parameters. However, it was found that a 3% variation in the gradients of the quadrupoles just upstream of the DTL produced agreement with the measured emittance growth. Unfortunately, this sensitivity was not seen in a later test in the machine.

Table 2 also shows the mismatch factors [2] calculated using the measured and simulated beam Twiss parameters. If the two beams were identical, the mismatch

factor would be 0. A few percent variation in some of the 140 quadrupole magnets of the DTL from the nominal operating gradients was required to produce a zero-mismatch. This is well within the known accuracy of the quadrupole gradients.

Table 2 - H^- 100-MeV Measurement and Simulation Results.

	Meas.	Simul.	MM.
$\epsilon_x(\pi - \text{cm} - \text{mrad}, \text{rms}, \text{norm})$	0.059	0.038	0.35
$\epsilon_y(\pi - \text{cm} - \text{mrad}, \text{rms}, \text{norm})$	0.042	0.034	1.07
$\epsilon_{x-\text{out}} / \epsilon_{x-\text{in}}$	3.2	1.8	
$\epsilon_{y-\text{out}} / \epsilon_{y-\text{in}}$	2.2	1.5	

C. Beam Loss at LAMPF

Simulations and operational data both show that the majority of beam loss after the DTL occurs at three locations along the linac: 1) In the transition region (TR), where the beam is transported from the DTL to the SCL at 100 MeV, 2) In module 5, at injection to the SCL at 100 MeV, and 3) near module 13, where the SCL transverse focusing becomes weaker by a factor of two (212 MeV). The simulations over-predict the absolute losses in the CCL by approximately an order of magnitude for the H^- beam and under-predict them by an equal amount for the H^+ beam when compared to the 1993 run cycle data. However, we feel that the simulations are a self-consistent set and that the trends they show will be seen in the real machine.

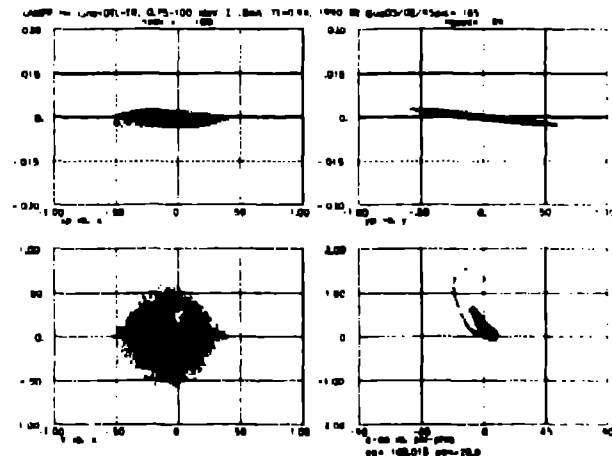


Figure 1: DTL output phase space and xy distributions at 100-MeV. The lower right plot is the longitudinal phase space. Note the long tail in the distribution.

The beam from the ion source is monoenergetic and unbunched. Before this beam is injected into the DTL, it must be bunched and matched transversely. The present two-buncher system in the low-energy beam transport line is not capable of 100% bunching of the beam. The fraction of the beam which lies outside of the longitudinal

acceptance of the DTL will not be captured or accelerated and will be lost in the DTL. This has been verified in the simulations. Figure 1 shows the DTL output distributions at 100-MeV from the simulations. The figure in the lower right is the longitudinal phase space plot. It should be noted that the particles which populate the tail of the longitudinal output distribution originated from the outer edge of the longitudinal acceptance, at injection, which is the nonlinear region of the phase space. Due to the factor of four decrease in the longitudinal acceptance at injection to the SCL (transition from 201.25-Mhz to 805-Mhz, some of these particles will be outside of the longitudinal acceptance of the SCL and will be lost there.

Simulation studies were used to determine the effect of the DTL tank amplitudes on the DTL output beam emittance at 100-MeV. It was found that there is a broad minimum in longitudinal emittance near 96% of design amplitude. During the 1993 run cycle, the DTL tank 1 amplitude was operated near 0.94 times the design value. The result is rather dramatic. A 6% reduction in tank 1 amplitude reduces the transmission by 30% and reduces the longitudinal emittance by 60%. The transverse output emittance is not affected.

Figure 2 shows the energy spectrum of only particles lost in the SCL from simulations. It can be seen that these particles have energies of 100 ± 5 -MeV. Figure 3 shows the energy spectrum of particles lost in both the TR and the SCL from simulations. This distribution has a low-energy tail with particle energies extending down to approximately 15-MeV. The particles in the low-energy tail are lost in the first two dipoles of the TR and therefore cause structure activation in the TR only. The remainder of the particles, with energies near 100-MeV, are not captured in the SCL. These particles are lost at the SCL entrance if they originated at the outer edge of the xy (transverse) distribution. Otherwise, because they are off-energy, some of these particles drift in the SCL until they are sufficiently deflected to the beam pipe or structure wall.

IV. A POSSIBLE UPGRADE PATH

We have done simulations where the first tank of the DTL was replaced with a 5.39-MeV RFQ and a bunch-rotator cavity was placed in the TR for longitudinal matching into the SCL for the H^+ beam. Fig 4 shows the DTL output distributions at 100-MeV from simulations with the RFQ. The longitudinal phase space plot is shown in the lower right corner and should be compared to Fig. 2. The longitudinal tail of the distribution is much reduced.

Because the beam is bunched adiabatically over many synchrotron oscillation periods in the RFQ, the bunching process is more complete. In the simulations, the DTL tanks were at full design amplitude and the simulated DTL transmission was found to be 100%. The simulated losses in the SCL were found to be 1.4% without longitudinal

matching into the SCL at 100-MeV. However, simulations including the effect of a single multi-gap bunch-rotator cavity in the TR reduced the SCL losses to 0.005%, compared to 1.2% for simulations of the existing machine. These simulations demonstrate the importance of good longitudinal capture and matching.

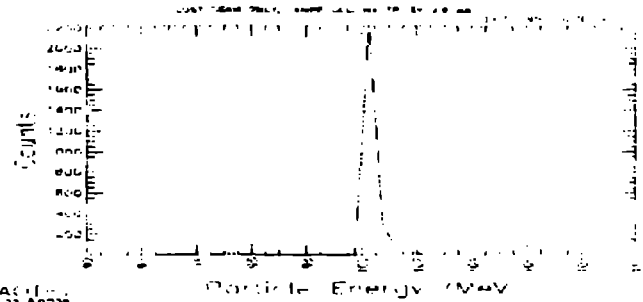


Figure 2: Energy spectrum of particles lost only in the SCL as determined from simulations.

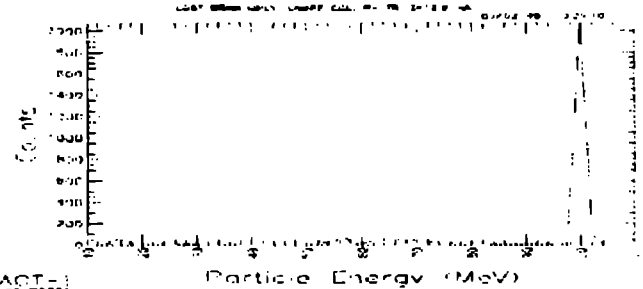


Figure 3: Energy spectrum of particles lost in the TR and the SCL as determined from simulations.

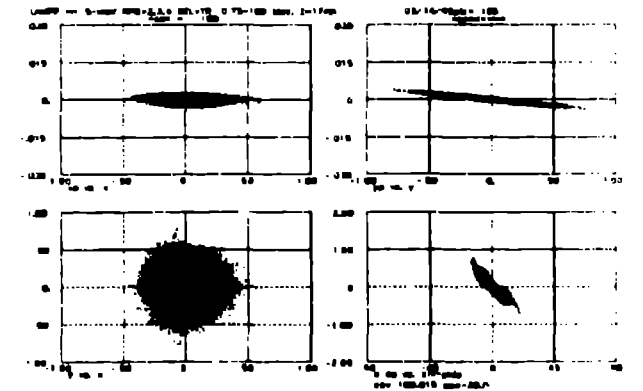


Figure 4: DTL output phase space and xy distributions at 100-MeV for the 5.39-MeV RFQ. Note the lack of a long tail in the longitudinal distribution.

IV. REFERENCES

- [1] R. W. Garnett, R. S. Mills, and T. P. Wangler, "Beam Dynamics Simulation of the LAMPF Linear Accelerator," Proceedings of the 1990 Linac Conference, Sept. 9-14, 1990, Albuquerque, NM.
- [2] K. Crandall, "TRACE 3-D Documentation," Los Alamos National Laboratory Report, LA-11054-MS (August 1987).

DISCLAIMER

This report was prepared as an account of work sponsored by an agency of the United States Government. Neither the United States Government nor any agency thereof, nor any of their employees, makes any warranty, express or implied, or assumes any legal liability or responsibility for the accuracy, completeness, or usefulness of any information, apparatus, product, or process disclosed, or represents that its use would not infringe privately owned rights. Reference herein to any specific commercial product, process, or service by trade name, trademark, manufacturer, or otherwise does not necessarily constitute or imply its endorsement, recommendation, or favoring by the United States Government or any agency thereof. The views and opinions of authors expressed herein do not necessarily state or reflect those of the United States Government or any agency thereof.